

Role of amniotic fluid mesenchymal cells engineered on MgHA/collagen-based scaffold allotransplanted on an experimental animal study of sinus augmentation

Paolo Berardinelli · Luca Valbonetti · Aurelio Muttini ·
Alessandra Martelli · Renato Peli · Vincenzo Zizzari ·
Delia Nardinocchi · Michele Podaliri Vulpiani ·
Stefano Tetè · Barbara Barboni · Adriano Piattelli ·
Mauro Mattioli

Received: 22 May 2012 / Accepted: 27 September 2012 / Published online: 14 October 2012
© Springer-Verlag Berlin Heidelberg 2012

Abstract

Objectives The present research has been performed to evaluate whether a commercial magnesium-enriched hydroxyapatite (MgHA)/collagen-based scaffold engineered with ovine amniotic fluid mesenchymal cells (oAFMC) could improve bone regeneration process in vivo.

Materials and methods Bilateral sinus augmentation was performed on eight adult sheep in order to compare the tissue regeneration process at 45 and 90 days after implantation of the oAFMC-engineered scaffold (Test Group) or of the scaffold alone (Ctr Group). The process

of tissue remodeling was analyzed through histological, immunohistochemical, and morphometric analyses by calculating the proliferation index (PI) of oAFMC loaded on the scaffold, the total vascular area (VA), and vascular endothelial growth factor (VEGF) expression levels within the grafted area.

Results MgHA/collagen-based scaffold showed high biocompatibility preserving the survival of oAFMC for 90 days in grafted sinuses. The use of oAFMC increased bone deposition and stimulated a more rapid angiogenic reaction, thus probably supporting the higher cell PI recorded in cell-treated sinuses. A significantly higher VEGF expression (Test vs. Ctr Group; $p=0.0004$) and a larger total VA ($p=0.0006$) were detected in the Test Group at 45 days after surgery. The PI was significantly higher ($p=0.027$) at 45 days and became significantly lower at 90 days ($p=0.0007$) in the Test Group sinuses, while the PI recorded in the Ctr Group continued to increase resulting to a significantly higher PI at day 90 (CTR day 45 vs. CTR day 90; $p=0.022$).

Conclusions The osteoinductive effect of a biomimetic commercial scaffold may be significantly improved by the presence of oAFMC.

Clinical relevance The amniotic fluid mesenchymal cell (AFMC) may represent a novel, largely and easily accessible source of mesenchymal stem cells to develop cell-based therapy for maxillofacial surgery.

P. Berardinelli · L. Valbonetti · A. Muttini · A. Martelli · R. Peli ·
D. Nardinocchi · B. Barboni · M. Mattioli
Department of Comparative Biomedical Science,
University of Teramo,
Teramo, Italy

V. Zizzari
Department of Drug Sciences, University “G. d’Annunzio”,
Chieti, Italy

M. Podaliri Vulpiani
Istituto zooprofilattico sperimentale “G. Caporale”,
Teramo, Italy

S. Tetè (✉) · A. Piattelli
Department of Medical, Oral and Biotechnological Sciences,
University “G. d’Annunzio”,
Chieti, Italy
e-mail: tete@unich.it

L. Valbonetti · A. Muttini · S. Tetè · B. Barboni
Stem TeCh group,
Chieti, Italy

Keywords MgHA/collagen-based scaffold · Amniotic fluid mesenchymal cells · Maxillary sinus augmentation · Preclinical setting · Sheep

Introduction

Maxillary sinus grafting has become a common procedure in preprosthetic reconstructive surgery [1–4]. Autogenous bone grafting has long been considered the gold standard for sinus augmentations [4–7]. Because of its main disadvantages, such as limited availability and donor site morbidity, various allografts, xenografts, and alloplastic biomaterials have been successfully used to substitute autogenous bone [3, 8, 9]. The different bone substitutes developed are characterized by an osteoconductive potential that is exerted through their ability to induce native bone growth [10–13]. Various osteoconductive biomaterials have been used for maxillary sinus grafting but due to the absence or scarcity of local osteoprogenitor cells in order to have complete bone regeneration at the site of sinus floor elevation, several months are required [14]. For this reason, new regenerative strategies are being continuously developed, mimicking as closely as possible nature, as demonstrated by the new generation biomaterials [15]. Wettability, texture, chemical composition, and surface topography are all biomaterial properties that have been improved to increase their interaction with native cells/tissue, and therefore, osteoinductivity [16–22]. However, the relatively long time required for bone healing treated with synthetic biomaterials represents a surgical limit in maxillofacial surgery, thus explaining the efforts of several research groups towards an innovative approach that combines the use of osteoinductive scaffolds and stem cell-based therapy. Tissue engineering applied to bone regeneration, however, opens two new integrated problems: firstly, it increases the requirement of biocompatible scaffolds that must guarantee stem cell adhesion, migration, proliferation, and differentiation and secondly, it requires a suitable stem cell source able to guarantee a safe, efficient, and extended process of new bone deposition [23]. Promising results have been achieved so far from the use of stem cells showing how these cells contribute significantly to the reestablishment of structure and functionality of a variety of injured tissues or organs. Although a lot of research has been focused on the ability of stem cells to differentiate within the injured areas, more recent research suggests that other relevant mechanisms are involved in supporting their regenerative effect, such as secretion of paracrine factors that stimulate endogenous cell differentiation and proliferation, modulation of injured tissue inflammation, and control of neovascularization. Among the many cell types proposed for regenerative medicine, mounting evidences suggested that amniotic fluid mesenchymal cells (AFMC) may represent an emerging source of stem and progenitor cells immensely valuable, easily accessible, and with biological properties particularly useful for the development of new protocols of stem cell-based therapy [24–28]. In primis, AFMC conjugate the absence of risk of tumor formation [25] with the capacity to differentiate

into multiple cell lineages (endo-, meso-, and ectodermal lineages) [30–34]. All the categories of amniotic-derived cells, in fact, arise early in gestation, during the pregastrulation stages of embryonic development, thus harboring stem–progenitor cells that display a plasticity and some degree of stemness that is typical of embryonic cells [25, 30–34]. In addition, from their fetomaternal tolerance role, amniotic cells seem to derive their immune-modulatory and antiinflammatory properties, which represent another valuable characteristic during the reparative processes of different tissues and a unique biological prerequisite to undertake clinical trials of allotransplantation in the absence of any immunosuppressive treatment [25]. Even if preclinical studies indicating the osteoregenerative properties of AFMC grafted into the common procedure of maxillary sinus lift are not available yet, several evidences indicate high osteogenic plasticity [35–41]. Starting from these premise, the present research was designed to assess whether a commercial magnesium-enriched hydroxyapatite (MgHA)/collagen-based scaffold that reproduces faithfully the architecture and biochemical properties of extracellular matrix of bone tissue [19, 20] could improve its therapeutic outcome when used in maxillary sinus augmentation procedures in combination with ovine amniotic fluid mesenchymal cell (oAFMC) and whether it could be able to support a consistent new bone tissue deposition in a reasonable time interval, comparable to that of current procedures [1–4]. Firstly, the experiments were designed to verify whether the scaffold was biocompatible with oAFMC under in vitro conditions, thus generating stable engineered biocomplexes to use for preclinical grafts. Then, using sheep as a validated experimental model for sinus lift procedures [42], the deposition of new bone tissue was assessed 45 and 90 days after the implantation of the MgHA/collagen-based scaffold alone (CTR) or engineered with 10 million oAFMC into the maxillary sinuses. The contribution of oAFMC to the process of osteogenesis was investigated by assessing the process of new bone formation, cell proliferation, vascular endothelial growth factor (VEGF) secretion, and total vascular area (VA) extension.

Material and methods

Biomaterial

For the present research, a commercial MgHA/collagen-based scaffold, the RegenOss[®], was used. The biomaterials is a nanostructured biomimetic scaffold (Fin-Ceramica Faenza S.p.A., Faenza, Italy) with a porous three-dimensional (3D) composite architecture, mimicking the complex hierarchically organized bone structure, obtained through a proprietary technique in which a specific hybrid organic–inorganic composite is spontaneously built, driven by biological mechanism (so-

called biomineralization). In particular, the biomaterial consists of a combination of type I collagen (30 %) and MgHA (70 %) (Fig. 1); it is synthesized using a standardized process starting from an atelocollagen aqueous solution (1 %, w/w) in acetic acid, isolated from equine tendon (Opocrin S.p.A., Modena, Italy). The mineralized structure is manufactured by nucleating bonelike nanostructured nonstoichiometric hydroxyapatite into self-assembling collagen fibers, as it occurs in the biological process of neossification [12].

Chemical agents

All chemical reagents and media used were purchased from Sigma-Aldrich Co. (St. Louis, MO, USA), unless otherwise specified.

oAFMC isolation and treatment

oAFMC isolation

oAFMC were collected from sheep fetuses at a local abattoir by removing the whole pregnant uterus and bringing it at 30 °C to the laboratory for further evaluation and processing. Only fetuses of 25–30 cm of length, at approximately 3 months of development were used [43]. Once opened, the uterus wall, ~100 ml of amniotic fluid was collected with a sterile 20-ml syringe through 18-gauge needle. oAFMC were centrifuged at 800g for 20 min and pelleted cells were seeded in a flask containing growth medium (Minimum Essential Medium Eagle Alpha Modification (α MEM) supplemented with 20 % fetal calf serum (FCS), 1 % ultraglutamine, 1 % penicillin/streptomycin plus 10 ng/ml FGF) at a concentration of 3×10^3 cells/cm². At 70–80 % confluence, dead cells and debris were removed with medium and the cells were dissociated by 0.05 % trypsin–ethylenediaminetetraacetic

acid (EDTA) and plated again at 3×10^3 cells/cm² for three consecutive expansion passages. Then, AFMC of each fetus were stored in vials of 2.5×10^6 in liquid nitrogen. Cryopreserved oAFMC were randomly thawed in order to test the effect of expansion in vitro on the: (1) hemopoietic, adhesion, stemness, and MHC marker expressions by cytofluorimetry and (2) the in vitro ability to differentiate into bone cell lineage.

Flow cytometer analysis of hemopoietic, adhesion, pluripotent, and MHC markers

Ovine AFMC derived from each fetus before and after thawing (third passage) were screened by flow cytometry in order to evaluate hemopoietic markers (CD14, CD31, and CD45), adhesion molecules (CD49f, CD29, and CD166), stemness intracellular markers (OCT4, SOX2, Nanog, and TERT), and MHC class I and II antigen expressions. The primary antibodies used for the analysis (Table 1) are commercially available. To optimize the antibody concentration by flow cytometry, sheep peripheral blood mononuclear cells (PBMCs) (positive control) were stained by hematopoietic markers (data not shown). Finally, cells were analyzed on a FACSCalibur flow cytometer (BD), using CellQuest™ software (BD). Flow cytometry measurement was carried out by using as quality control Rainbow Calibration Particles (six peaks) and CaliBRITE beads (both from BD Biosciences). Debris was excluded from the analysis by gating on morphological parameters (lymphocyte gate); 20,000 nondebris events in the morphological gate were recorded for each sample. All antibodies were titrated under assay conditions and optimal photomultiplier (PMT) gains were established for each channel. Data were analyzed using FlowJo™ software (Tree Star Inc., Ashland, OR, USA). Mean fluorescence intensity ratio (MFI ratio) was calculated by dividing the MFI of positive events by the MFI of negative events.

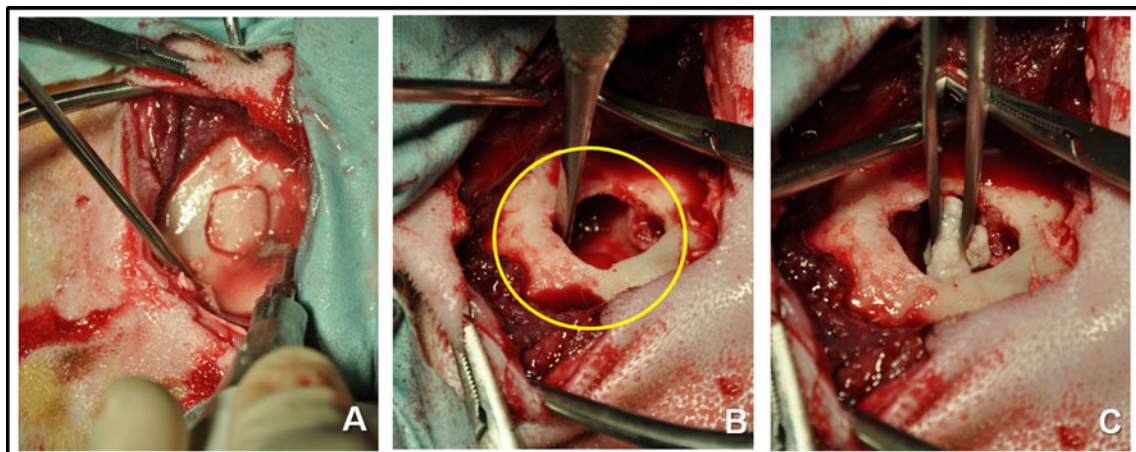


Fig. 1 Surgical steps of sinus lift experimental procedure: **a** surgical access through the maxillary bone performed by piezoelectric unit; **b** the hole across the maxillary bone identified by a circle; **c** insertion of RegenOss® scaffolds into the maxillary sinus under the lift Schneiderian membrane

Table 1 Primary antibodies of flow cytometry analysis

Antigen	Conjugated-fluorescent probe	Company details	
Hemopoietic markers			
CD14	FITC	LifeSpan BioSciences	Seattle, WA, USA
CD31	FITC	AbD Serotec	Oxford, UK
CD45	FITC	AbD Serotec	Oxford, UK
Adhesion molecules			
CD29		VMRD	Pullman, WA, USA
CD49f		Beckman Coulter	Fullerton, CA, USA
CD166	FITC	Ancell	MN, USA
MHC antigens			
Class I		Novus Biologicals	Cambridge, UK
Class II	HLA-DR	Abcam	Cambridge, UK
Stemness markers			
CD117		Abcam	Cambridge, UK
SOX2		Abcam	Cambridge, UK
OCT4	PE	Becton Dickinson	BD, San Jose, CA, USA
TERT		Calbiochem	Gibbstown, NJ, USA
NANOG		Chemicon Int'l.	Billerica, MA, USA

Osteogenic *in vitro* differentiation

Plasticity of oAFMC to differentiate into bone cell lineage was assessed on samples of thawed oAFMC by using validated cultural conditions [43, 44]. Thawed cells were seeded at the concentration of 2×10^4 cells/cm² in 25-mm petri dish fitted with a round glass coverslip and cultured in 2 ml of growth medium until they approached confluence. Then, half of the cells were maintained in growth medium while the remaining were incubated in osteoinductive medium (α MEM supplemented with 50 μ M ascorbic acid, 10 mM β -glycerol phosphate, 0.2 μ M dexamethasone, and FCS reduced to 10 %). Both cultures were incubated for 21 days before detecting the osteogenic differentiation with the Alizarin red staining and the alkaline phosphatase (ALP) assay. In detail, Alizarin red staining was performed on fixed cells (4 % paraformaldehyde for 15 min). Following a rinse with distilled water, the cells were incubated in 40 mM Alizarin red S for 30 min at room temperature and then quickly washed with 80 % acetone. Glass coverslips were finally rinsed in phosphate buffered saline (PBS) mounted on glass slides and analyzed on a phase-contrast microscope (Nikon Eclipse 600). Histochemical detection of ALP was revealed by cytochemical staining with 5-bromo-4-chloro-3-indolyl phosphate/nitro blue tetrazolium (BCIP/NTB, Liquid System, Sigma-Aldrich Co. St. Louis, MO, USA). Plated cells were fixed in precooled 4 % paraformaldehyde for 10 min, rinsed with deionized water and then incubated with BCIP/

NTB liquid system for 2 h at 37 °C temperature in the dark. The reaction was stopped by removing the substrate solution, the coverslips were washed in distilled water mounted on a glass slide, and the cells were analyzed with a phase-contrast microscope (Nikon Eclipse 600).

oAFMC loading on scaffolds

Thawed oAFMC, showing a stable phenotype and a conserved *in vitro* ability to undergo osteogenic differentiation, were labeled for 30 min with the fluorescent lipophilic dye, PKH26, according to manufacturer's instructions. PKH26 is stably incorporated in lipid regions of the cell membrane allowing *in vivo* cell tracking and monitoring studies [44–46]. The PKH26-labeled oAFMC (10×10^6) were seeded on single RegenOss®. Single engineered scaffolds were then incubated over a roller apparatus (Wheaton, Millville, NJ, USA) at 38 °C in 5 % CO₂ and air, and in order to achieve a widespread scaffold loading, culture was prolonged under agitation for 3 days at a speed of 6 rpm. At the end of the incubation, some scaffolds were analyzed to assess the loading efficiency while the remaining ones were used for the sinus augmentations procedures. Cell viability was assessed by incubating the loaded scaffolds with the vital cytoplasmic fluorescent dye calcein-AM. The incidence of proliferating cells was, in addition, detected by using Ki67. The cells were counterstained with 4',6-diamidino-2-phenylindole (DAPI) and visualized under an epifluorescent microscope.

Preclinical settings

Animal

The Ethical Committee of the Universities of Teramo and Chieti-Pescara approved the present research (Prot. n. 05/CEISA/PROG/32) performed on eight adult sheep, 2 years old, and 40–50 kg of weight. The sheep were bred according to the European community guidelines (E.D. 2010/63/UE). After 2 weeks of animal quarantine, surgical procedures were carried out in an authorized veterinary hospital. The animals were daily followed in the postsurgical period and the evolution of sinus transplantation was documented weekly by ultrasound analysis. The animals were then randomly divided into two different groups and euthanized to explant grafted sinuses at 45 and 90 days, respectively.

Sinus augmentation surgical procedure

The sheep were operated in lateral recumbency, under general anesthesia. Sedation was obtained with xylazine (0.2 mg/kg i.m; Rompun®; Bayer), diazepam (0.2 mg/kg

i.v.; Diazepam® 0.5: Intervet), and atropine sulfate (6 mg i.m.; atropine sulfate; Fort Dodge). Anesthesia was induced with ketamine (10 mg/kg i.m.; Ketavet® 100; Intervet) followed, after endotracheal intubation, by inhalation of 2.5 % halothane (Halotane®; Merial) in oxygen for maintenance. A bilateral sinus augmentation procedure with an extraoral approach was performed, as showed in Fig. 1. After careful preparation for sterile surgery, maxillary sinus was exposed ventrally to the lower orbital rim by a sagittal skin incision (1 cm dorsal and 1 cm caudal to tuber facial tuberosity). The masseter muscle and the adherent periosteum were separated by blunt dissection before preparation of an oval anrostomy. The osteotomy was carried out using a piezoelectric unit surgery (BioSAFin Easy Surgery, Ancona, Italy). A rectangular bony window (1.5 cm×1.0 cm) was created in the maxillary sinus wall under constant saline cooling and the resultant bone plate was gently removed from the Schneiderian membrane. The membrane was then gently elevated, by detaching it from the buccal, caudal, and medial bones and moving it cranially with bent blunt dissectors. The cavity obtained between the mucosa and the inferior osseous septum of the sinuses was augmented with two RegenOss® scaffolds each. Placement of scaffolds formerly seeded with 10×10^6 PHK26-stained oAFMC or of unseeded scaffolds was performed in the two sinuses in each animal (Fig. 1). The side of seeded and unseeded scaffold placement was randomly assigned. At the end of surgery, muscle planes, subcutaneous, and skin were layered and sutured. Postoperatively, the animals were given 20 mg/kg of ampicillin i.v. (Vetamplius®, Fatro) every 12 h for 3 days. The wounds were inspected daily for clinical sign of complications. Ultrasound examination was carried every 7 days on each surgical site. The study was performed with a Toshiba Nemio 20 (Toshiba Medical Systems Corporation, Otawara, Japan) equipped with a linear probe at 7.5 MHz (multifrequency 6/12 MHz). Due to the docile nature of the animals, a manual restraint was sufficient for the noninvasive examination. Animals were randomly divided into two groups to be euthanized 45 or 90 days after surgery by an overdose of thiopental (Pentothal Sodium, Intervet) and embutramide (Tanax®, Intervet).

X-ray

After sacrifice, a specimen comprising of the grafted area was cut by a bone saw in each animal, with sawing direction parallel to transversal plane of the skull. Then, each specimen underwent radiographic examination through portable X-ray equipment with a high frequency generator (20 mA/90 kV) (Franceschini Angelo, Bologna, Italy).

Morphological analysis of sinus explants

Sinus explants (woven blocks of $\sim 4.5 \text{ cm}^3$ in size; Fig. 1b) were fixed in 4 % paraformaldehyde solution (PBS, pH 7.4) before processing for histological and immunohistological analyses.

Histological analysis

The explants were decalcified for at least 20 days in 14 % EDTA before freezing in 30 % sucrose–PBS. The explants were completely cryosectioned at 10- μm thickness. The morphological and morphometric analyses were performed on eight serial sections collected every $\sim 300\text{-}\mu\text{m}$ distance. Two sections were stained with hematoxylin–eosin (HE) to describe the architecture of new formed tissues.

Immunohistological analysis

Six serial cryosections were immunostained against: (1) Ki67, in order to describe the proliferation index (PI) of oAFMC loaded on the scaffold, as well as that of the cells within the host tissues; (2) von Willebrand factor (vWF), to quantify the total VA; and (3) VEGF, in order to detect the synthesis of the major angiogenic growth factor. Immunohistochemical analyses were performed as previously described [47, 48]. Briefly, mouse anti-Ki67 (diluted 1:10 in PBS/1 % bovine serum albumin (BSA); Oncogene), rabbit anti-vWF (diluted 1:400 in PBS/1 % BSA, Dako, Glostrup, Denmark), and rabbit anti-VEGF were applied at room temperature overnight after hot-box oven at 95 °C for 5 min twice. The tissue sections were then incubated with biotinylated secondary antibody: for the Ki67, a biotinylated-conjugated goat anti-mouse antibody (diluted 1:100 in PBS and applied for 1 h; Sigma-Aldrich Co.) was used while the vWF and VEGF immunocomplexes were visualized by using a biotinylated-conjugated goat anti-mouse antibody (1:100 in PBS; Sigma-Aldrich Co.). The immunoreaction was detected using fluorescein isothiocyanate (FITC)-labeled avidin complex. According to the data sheet instructions, bovine aorta tissue collected at the slaughterhouse and human breast carcinoma tissue samples were used as positive control. Normal goat serum was used as negative control in place of primary antibodies. Tissue sections were counterstained with DAPI (Vectastain, Burlingame, CA, USA) in order to visualize cell nuclei.

Morphometric analyses

Immunofluorescence analyses were performed to calculate the PI, total VA, and VEGF expression levels within the grafted area. The analyses were carried out by using an Axioskop 2 plus (Zeiss, Oberkochen, Germany), equipped with a digital camera (Axiovision Cam, Zeiss, Oberkochen,

Germany), and the data were processed by a KS300-computed image analysis system (Zeiss), as previously described [49]. The analyses were performed on at least five different sections/sinuses, and at least eight different fields/sections were blinded evaluated. The PI, total VA, and VEGF expression were quantified at $\times 200$ magnification and the digitized fluorescent vessel signals (fluorescent-positive area) were accomplished using a semiautomated algorithm. The total VA was calculated as square micrometer of vWF-positive area/field ($15,000 \mu\text{m}^2$). The PI was expressed as the percentage of Ki67-positive cells/total cells and the expression of VEGF was calculated as square micrometer of the VEGF-positive area/field as previously described [49].

oAFMC retrieval in sinus explants

The presence of PKH26 labeled oAFMC was ascertained by analyzing the cryosections, preliminarily stained with DAPI to counterstain cell nuclei, under the Axioskop 2 plus microscope (Zeiss, excitation: 551 nm, emission: 567 nm).

Statistical analysis

To compare the effect exerted by different treatments, the data were checked for normal distribution by D'Agostino and Pearson's test and were compared by a two-way

ANOVA test. Finally, the post hoc Tukey test (GraphPad Prism 5) was carried out in order to evaluate the “individual” effect on each examined variable.

Results

oAFMC isolation and molecular characterization

After three passages in vitro, cells isolated from amniotic fluid appeared as a uniform population of fusiform cells. The oAFMC expanded in vitro, after cryopreservation, and did not modify their molecular profile as summarized in Fig. 2a. In detail, oAFMC did not express the hemopoietic markers CD14, CD31, and CD45, analogously at the stemness marker CD117 and the MHC class II. Independently from cryopreservation, the adhesion molecules CD29, CD49f, and CD166 were lowly expressed such as the MHC class I molecules and the stemness marker Oct3/4. By contrast, the three stemness markers TERT, Nanog, and Sox-2 were largely expressed and their profiles were not affected by cryopreservation. Thawed oAFMC maintained a prompt ability to undergo osteoblast cell lineage differentiation as indicated by the intense extracellular matrix mineralization visualized by Alizarin red staining and by the large ALP activity recorded in cells cultured for 21 days in osteoinductive media (Fig. 2b).

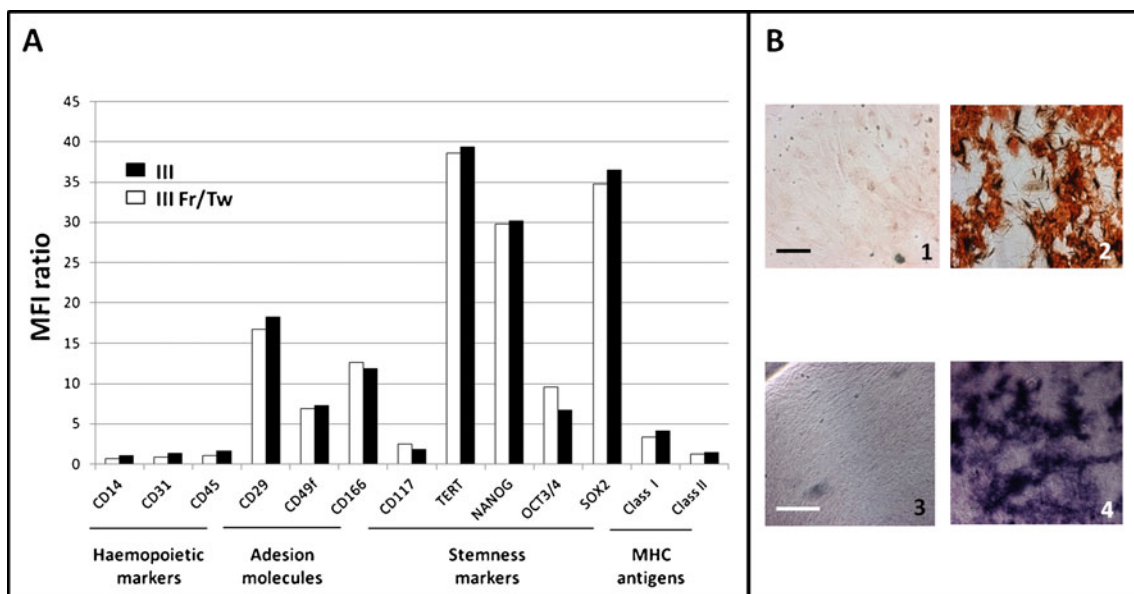


Fig. 2 a Histograms show the average of MFI ratio levels detected for surface, MHC, and stemness markers analyzed on three replicates of thawing oAFMC after three passages of in vitro expansion by flow cytometry. Standard deviation never exceeded 5 %. b In vitro

osteogenic plasticity of thawed oAFMC assessed after 21 days of culture in growth of osteoinductive media (2–4 and 1–2, respectively) by using Alizarin red (top images) and ALP assay (bottom images). Scale bars=50 μm

oAFMC-engineered scaffold

The MgHA/collagen-based scaffold showed high ability to support oAFMC adhesion and proliferation. In fact, after 3 days of incubation, the scaffolds were completely covered by live oAFMC (Fig. 3), as demonstrated by the intracellular retention of calcein-AM dye. Only a low percentage of cells did not attach to the scaffold and were recovered in the culture medium ($\sim 1\text{--}3\%$ of 10×10^6 cells/scaffold/petri dish). Several oAFMC found on the scaffold showed, in addition, Ki67-positive nuclei, thus indicating the persistence of a favorable environment for cell division (Fig. 3).

Sinus augmentation clinical procedure

For their texture and flexibility, the scaffolds were easily inserted within the maxillary sinus, where they could be adapted to the irregular sinus cavity without problems. The recovery from anesthesia and the convalescence period were uneventful and none of the animals showed signs of discomfort.

Ultrasound examination

Weekly, ultrasound scans allowed us to follow the process of tissue regeneration within the grafted sinuses. After

1 week, both treated sinuses, one grafted scaffold seeded with 10×10^6 PHK26-stained oAFMC and the other grafted with the scaffolds alone, appeared similar, as a round area (Fig. 4) of uniform echogenicity. The process of tissue regeneration was characterized, up to the seventh week, by the same (or increased) echogenicity that almost completely filled sinuses in a group transplanted with engineered scaffolds. On the contrary, starting from the fourth week, the sinuses treated with the scaffold alone displayed decrease of echogenicity in the grafted area, which showed irregular scattered echoes (Fig. 4). It was impossible to perform an effective examination from the seventh week due to the presence of organized reparative tissue covering the acoustic windows.

X-ray analysis

From the initial eight animals, one sheep was discarded for infection from the 45-day group, so another animal from the 90-day group was randomly excluded from the experimental study. In all animals euthanized after 45 days, the scaffolds were visible within the not oAFMC-seeded site (Fig. 5). By contrast, the biomaterial was completely embedded within a fibrous matrix in sites treated with the oAFMC-engineered scaffold (Fig. 5). However, no traces of scaffold were observed after 90 days, independently of the treatment considered (data not shown). Radiological analyses performed on

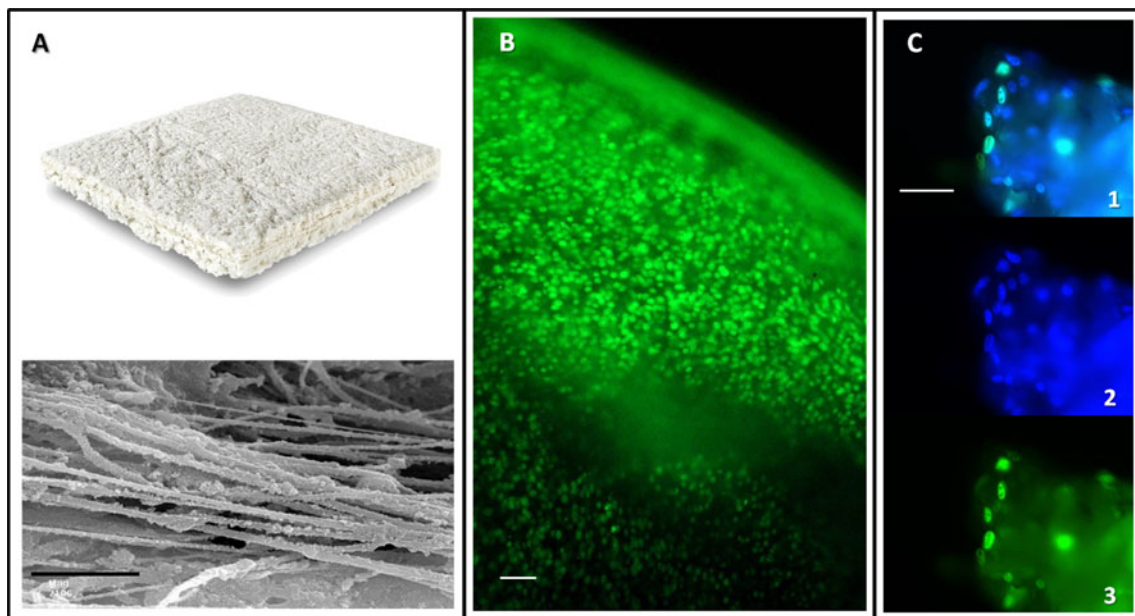


Fig. 3 **a** Macroscopic (*top*) and ultrastructural images (*bottom*) of RegenOss[®] of MgHA/collagen composite microstructure. Black scale bar=1 μm . **b** An example of the RegenOss[®] scaffold after 3 days of coincubation with 10×10^6 oAFMC. The cells have completely covered the surface of the scaffold as indicated by the calcein-AM dye that

resulted in entrapment within the cytoplasm of live cells. White scale bar=20 μm . **c** Immunohistochemistry was performed in order to identify, among the AFC (2 blue nuclei counterstained with DAPI) attached to the surface of RegenOss[®], the Ki67-positive cells (3 *green fluorescence: 1 merge*). White scale bar=50 μm

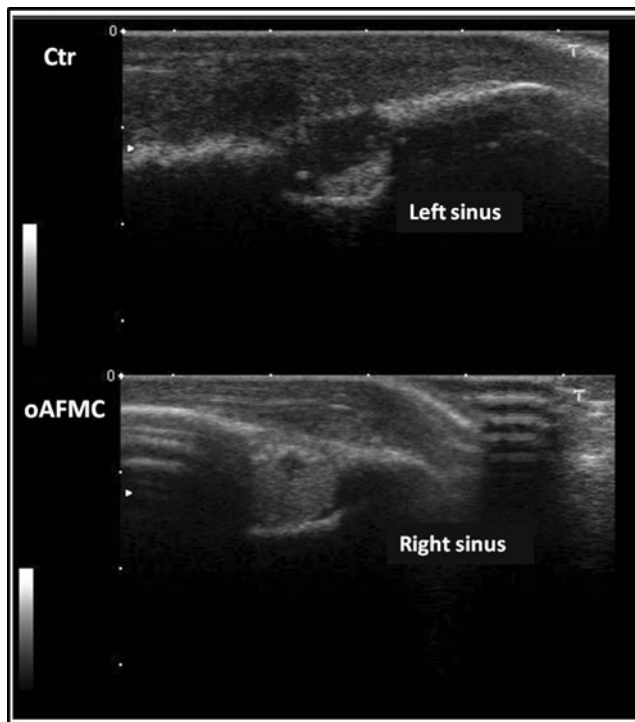


Fig. 4 An example of ultrasound analysis performed on RegenOss® (Ctr) and engineered RegenOss® (oAFMC) grafted sinuses performed 14 days after sinus augmentation surgical procedures

sheep following euthanasia allowed us to compare the content of the maxillary sinuses as showed in Fig. 5. In the three sheep from each group, those sacrificed after 45 and the other after 90 days from graft insertion, the X-ray analysis

revealed a dense area localized on the floor of the maxillary sinus in the oAFMC-engineered scaffold group (Fig. 5). These radiographic shadows had irregular margins and a density similar to that of the surrounding bone tissue, while in the group treated through the scaffold alone, no radiographic difference from a normal sinus floor was appreciable. To date, there is no published data regarding an objective score to evaluate the bone deposition in similar situations; however, differences between the two grafted sites are clearly detectable in the same radiographic image (Fig. 5).

Morphological analysis and oAFMC retrieval

In all the sectioned sinuses, the foci of newly deposited lamellar bone were mainly distributed at the periphery of the area grafted with the MgHA/collagen-based scaffold. In particular, new bone deposition was concentrated near the surgical incision and close to the native floor of maxillary sinus (data not shown). Osteogenesis was analogously activated in the oAFMC-engineered scaffold group (Fig. 6). However, in these samples, osteogenic foci were widespread within the grafted area even if they remained more active at the scaffold periphery (Fig. 6). In particular, several lamellar of newly deposited bone tissue filled the surgical access, while single and irregular foci matrix surrounded by active osteoblasts was found in the center of the grafted area (Fig. 6). A large proportion of PKH26 oAFMC was observed within the sinuses grafted with the engineered scaffolds (Fig. 6). The oAFMC were easily recognized by the red lipophilic dye

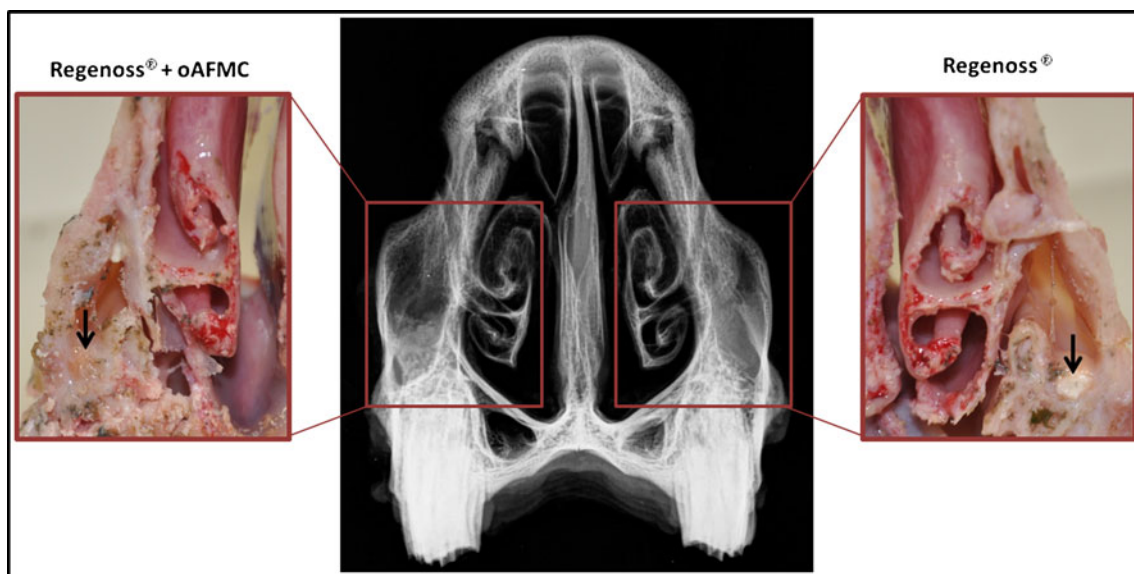


Fig. 5 An example of X ray analysis (*central image*) performed after 45 days on the explanted sheep head (*lateral windows*). The RegenOss® was clearly evident within the maxillary sinus grafted with the scaffold alone (*black arrow in the right box*) while appearing enclosed

within a fibrous matrix in the controlateral ones (oAFMC-implanted sinus: *arrow in the left box*). In this portion, an area of higher radio-density localized on the floor of maxillary sinus was observed

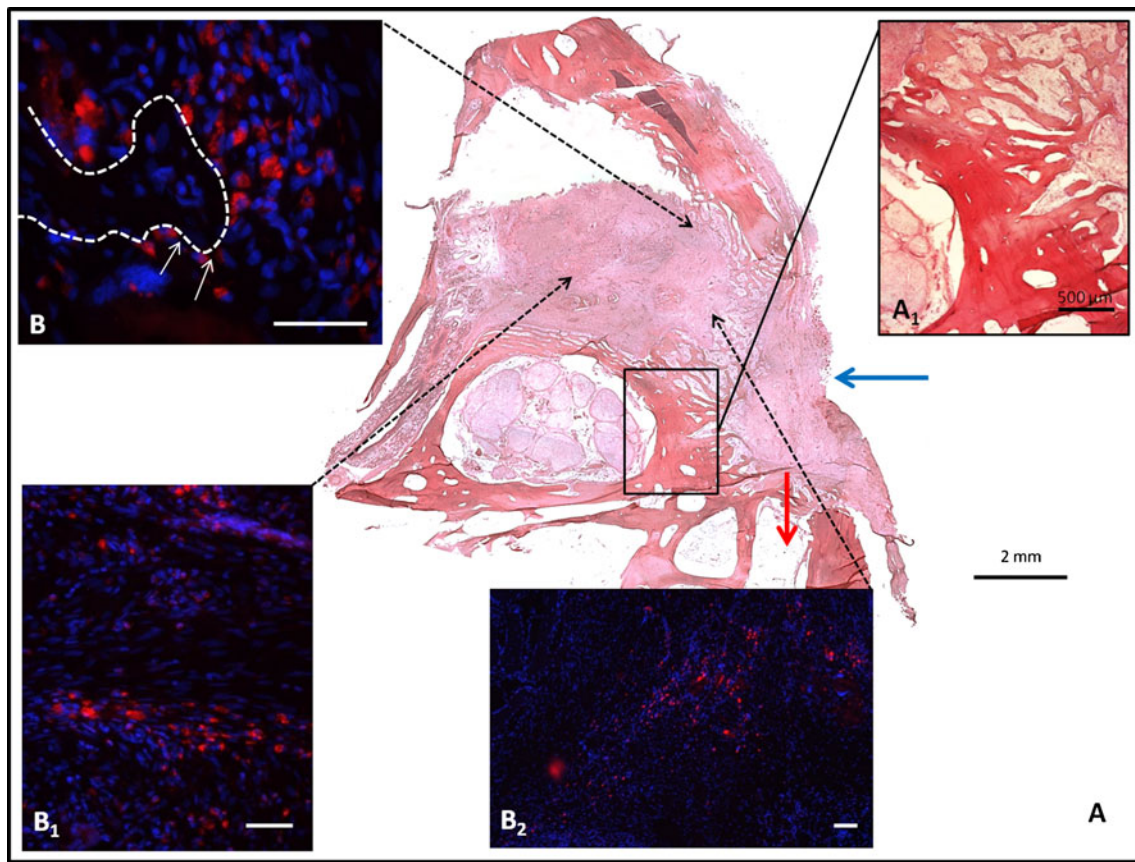


Fig. 6 *A* An example of a HE-stained section performed 45 days after the transplantation of oAFMC-engineered RegenOss® scaffold. The red arrow identifies the dental portion of maxillary sinus floor and the blue arrow, the surgical incision area. *A*₁ A higher magnification of the HE image showing the new deposition of trabecular bone. *B*, *B*₁, *B*₂

Images of increasing magnification showing the PKH26-positive cells distributed in different zones of the implanted area. The white dashed line indicates an area of newly deposited bone matrix surrounded by PKH26-positive cells, some displaying a fusiform osteoblastlike shape (white arrows). White scale bars=50 μm

localized at the periphery of bleu-counterstained nuclei (Fig. 6). They were largely integrated with the host tissue distributed among the fibrous matrix (Fig. 6), surrounding the foci of newly deposited matrix (Fig. 6) and close to the blood vessel network running in the grafted area. After 90 days, the amount of newly deposited bone further increased after 90 days (Fig. 7). In detail, mature bone was observed in the floor of both maxillary sinuses while lamellar bony tissue completely filled the surgical incision (Fig. 7b and c). The skeletal base of the maxillary sinuses treated with the engineered scaffold appeared more thickened than those recorded in untreated sheep (Fig. 7a). Several PKH26 oAFMC were still recorded 90 days after surgery, widespread within the grafted area (data not shown).

Morphometric analysis

A more intense angiogenic response was recorded within the sinuses grafted with oAFMC-engineered scaffolds as indicated by immunohistochemical analysis. In fact, a significantly higher secretion of VEGF ($p=0.0004$ oAFMC vs.

Ctrl Group) and a larger, parallel total VA ($p=0.0006$; Fig. 8) were detected in sinuses treated with oAFMC-engineered scaffold 45 days after surgery. Then, the angiogenic response decreased in both treatment groups although it was more marked in the oAFMC-engineered scaffolded ones where the extension of the total VA was significantly lower. Analogously, the PI recorded within the grafted area was influenced by the presence of oAFMC: the PI was, in fact, significantly higher in sinuses treated with oAFMC-engineered scaffolds at day 45 ($p=0.027$ oAFMC vs. Ctrl Group) and became significantly lower at 90 days ($p=0.0007$ oAFMC vs. Ctrl Group). By contrast, the PI recorded within the sinuses grafted with the scaffold alone continued to increase (Fig. 8), becoming significantly higher at day 90 ($p=0.022$ Ctrl day 45 vs. Ctrl day 90).

Discussion

The standard surgical procedure for maxillary sinus lifting consists of filling the cavity under the raised Schneiderian membrane with either autologous bone or biomaterials, or

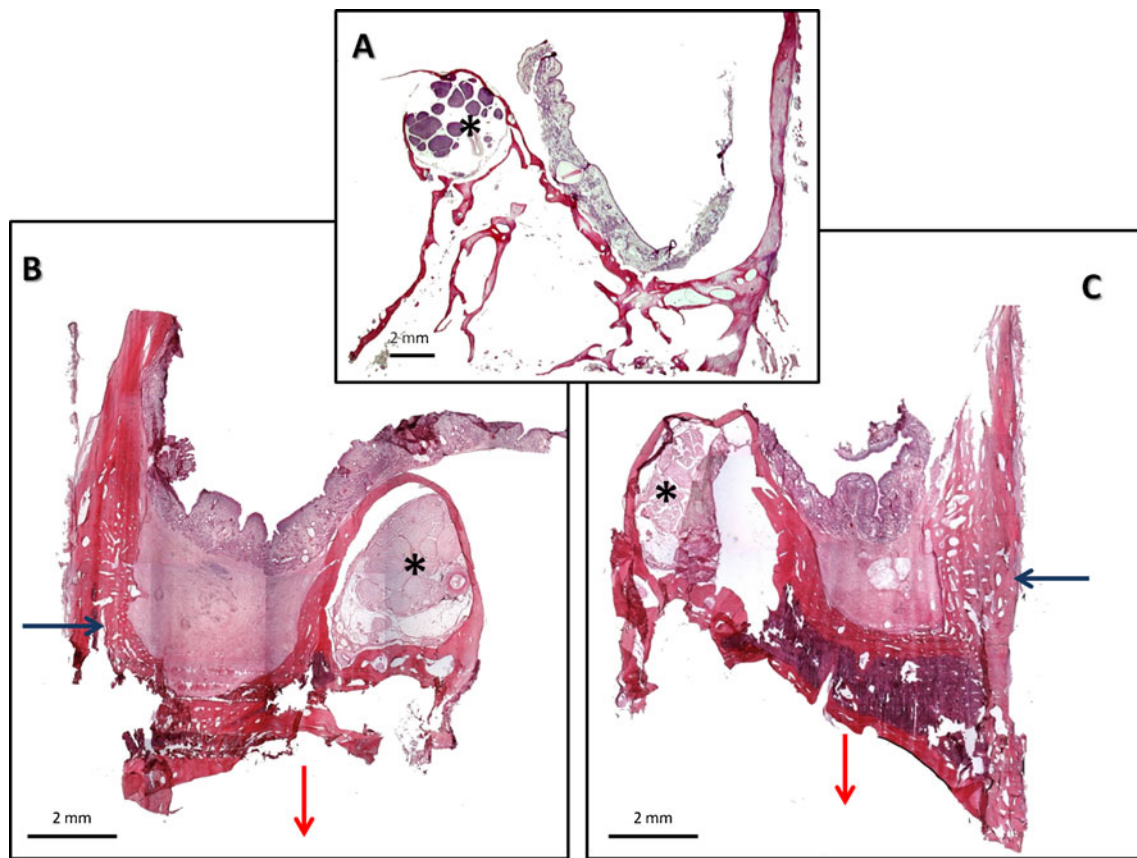


Fig. 7 **a** An example of a HE-stained section of an untreated ovine maxillary sinus. **b** and **c** are two examples of transplanted sinuses after 90 days from sinus lift procedures. **b** Sinus implanted with RegenOss® showing the surgical incision area filled with trabecular bone (blue arrows) and a thickened maxillary floor (red arrow). The implanted area localized under the elevated Schneiderian membrane is filled with

abundant fibrous tissue. **c** Sinus transplanted with engineered RegenOss® displaying the entire basis of the skeletal maxillary sinus greatly thickened. Abundant trabecular bone is accumulated within the surgical incision (blue arrow), while a more mature bony tissue is organized on the maxillary floor (red arrow). The asterisks indicate the infraorbital nerve

the combination of the two. Clinicians are constantly searching for a heterologous bone substitute that combines the osteoregenerative features of autologous bone overcoming limits connected to its use, such as the scarce availability of autologous bone and the high donor site morbidity [3–5, 8]. Therefore, innovative methods including the use of alternative biomaterials in combination or not with stem/progenitor cells have been recently investigated [10, 11, 20]. At present, tissue engineering is the most promising strategy to repair large bone defects [5, 50–53]. First of all, tissue engineering requires porous scaffolds that allow progenitor and differentiated cells to adhere, proliferate, and differentiate. This biocompatibility is a prerequisite for engineering the scaffold with live cells and, at the same time, it represents the condition by which it expresses osteoinductive activity once grafted in host tissues. Previous investigations demonstrated that for its structural and chemical compositions, RegenOss® is a suitable biomimetic nanostructured matrix for bone regeneration [20–22]. The present research extends its potential clinical applications, showing that the scaffold manifests osteoinductive properties

also when placed in the maxillary sinus. In vitro cell seeding showed that RegenOss® could completely support oAFMC adhesion and proliferation. The surface of the commercial MgHA/collagen-based scaffold was, in fact, able to entrap a very high concentration of cells (10×10^6 cells/cm²) when maintained under dynamic cultural conditions for 3 days. The adhesion of oAFMC did not appear to be a passive event, since attached cells elongated on the scaffold structure and a percentage underwent active mitosis. For this reason, we decided not to use more complex methods to establish the efficiency of loadings as frequently adopted when bioavailability of different biomaterials is compared. The biocompatibility of the scaffold was then confirmed in vivo by the high degree of tissue integration and the prompt osteogenic effect recorded in grafted sinuses. In this context, it was interesting to notice the clear osteoconductive potential that created a framework upon which osteoprogenitor cells could spread from the margins of the defect and generate new bone. In addition, our data show that all host tissue responses were clearly improved by the presence of grafted cells. In fact,

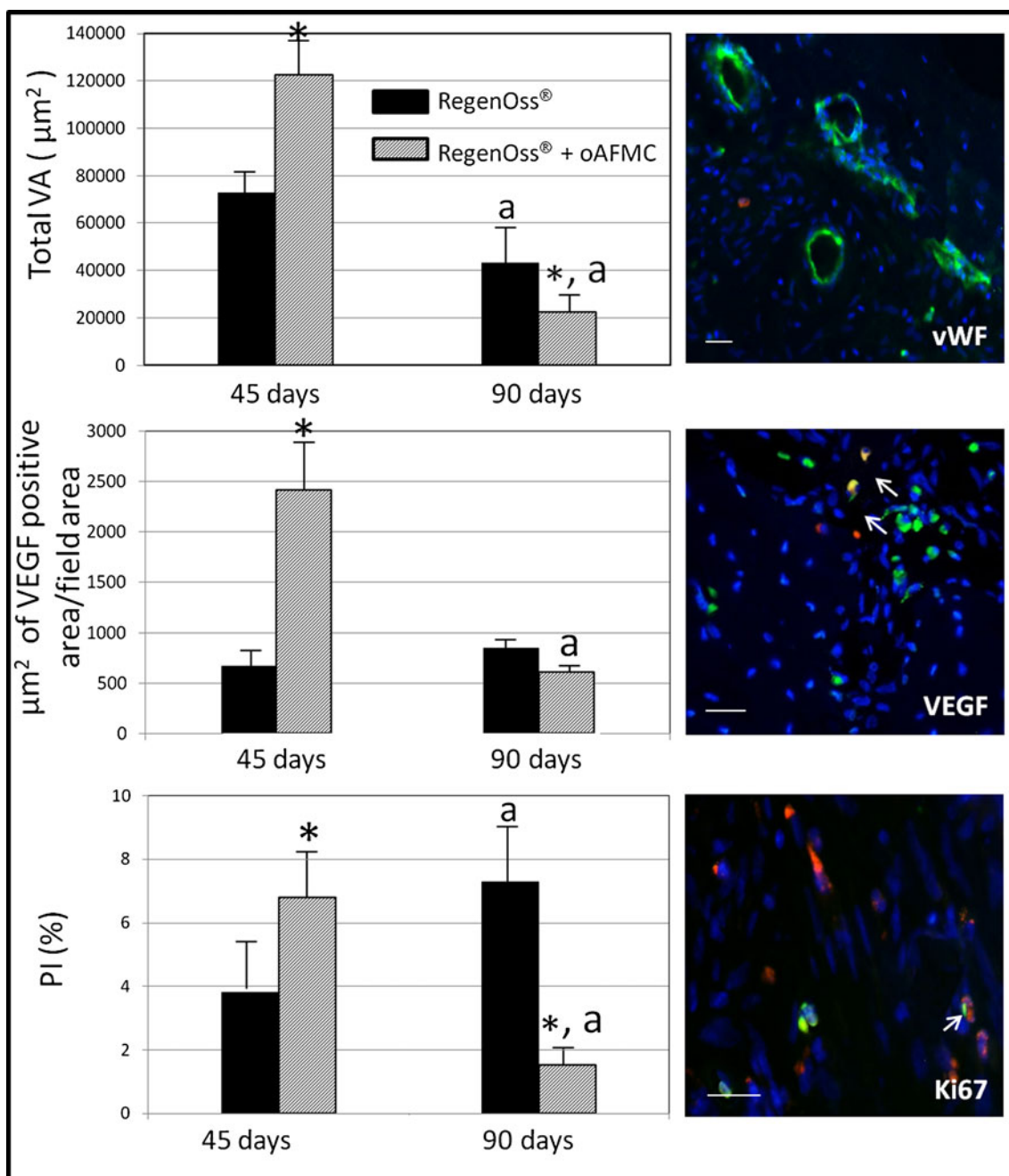


Fig. 8 a The histograms show the evolution of total VA, VEGF expression, and PI within the implanted districts. The data are expressed as mean±S.D. *Asterisk* data of Ctr- and oAFMC-treated sinuses that resulted in a significant difference for $p < 0.01$ when compared within the same interval time (i.e., Ctr day 45 vs. oAFMC day 45). *a* Data of Ctr- or oAFMC-treated sinuses that resulted in a significant difference for $p < 0.05$ when compared between the two

different interval points (i.e., Ctr day 45 vs. Ctr day 90). **b** Three examples of immunohistochemistry analysis performed to quantify the endothelial-positive area marked with the von Willebrand Factor (vWF), the VEGF expression, and the PI detected by the mitotic marker Ki67. The *white arrows* indicate PHK26-positive oAFMC that coexpress VEGF (*middle image*) and Ki67 (*bottom image*) molecules. White scale bars=50 µm

oAFMC accelerated bone deposition as well as other mechanisms of tissue regeneration, thus demonstrating their potential in regenerative medicine. For the first time, oAFMC has been used with success in a preclinical setting of sinus augmentation. Different sources of MSC have been previously considered as attractive for the maxillofacial surgery, such as

adipose tissue, dental pulp, or bone marrow [5], and the cells expressed a prompt osteogenic phenotype when incubated under adequate in vitro conditions [5, 50–54]. However, amniotic-derived cells may offer some additional biological properties that could be particularly useful to develop new protocol in regenerative medicine [14]. Amniotic fluid, rich in

mesenchymal-like cells [27–30], can be easily collected during prenatal diagnosis amniocenteses without raising any ethical problem [24–30]. In addition, oAFMC, like other amnion-derived cells, display a high differentiation capacity toward all three germ layers demonstrated both under *in vitro* and *in vivo* conditions [31–33, 43–46] either as native cell population or better as CD117-sorted cells [31]. Due to this pluripotency and to the early embryonic origin, the amniotic-derived cells are considered as fetal cells showing a degree of stemness that is typical of embryonic stem cells, even if they lack either tumorigenicity or immunogenicity [24]. The present research demonstrated that oAFMC could differentiate *in vitro* into osteoblastlike cells, as previously reported for human AFMC [35–41]. In fact, osteogenesis occurrence was clearly demonstrated after 3 weeks of culture in an osteogenic medium by the extensive mineralization of the extracellular matrix and by the large expression of ALP. Although several experimental evidences showed that a variety of stem cells can consistently differentiate *in vitro* into different cell lineages, their fate after transplantation and particularly their contribution to tissue regeneration in the host animal remains still largely unknown. Transplanted stem cells could, in fact, contribute directly to tissue regeneration by differentiating into the cell lineage of the damaged tissue or, indirectly, by creating favorable conditions for the repair process such as an adequate local angiogenic reaction. In the vast majority of successful preclinical trials so far carried out [24–31], the nature of the regenerative effects exerted by amniotic-derived stem cells has not been identified. Two major prerequisites for any therapeutic effect to be manifested are the presence of the cells in the lesion zone and the time interval of their survival in the host tissue. The present investigation offers an interesting feedback in this regard. A large number of transplanted cells could, in fact, be detected to be spread in the lesion. Moreover, the distribution of red-stained membrane surrounding the nuclei indicate that oAFMC survive for up to 90 days. It is probably thanks to this extended presence in the sinuses that oAFMC could exert their beneficial regenerative influence. This influence appears to result from the combination of at least three major components: (1) a direct contribution to osteogenesis, (2) a finely tuned local angiogenic response, and (3) a high cell proliferation in regenerative-grafted sinuses. The osteoinductive properties of RegenOss® were, in fact, improved by oAFMC that markedly accelerated the process of new bone deposition. The microscopic evaluation of the explants demonstrated that while the foci of bone deposition at day 45 were exclusively localized at the periphery of the area grafted with the MgHA/collagen-based scaffold alone, the presence of cells guaranteed a more widespread presence of bony foci that were observed also in the central portion of the sinus cavity. After 90 days, the beneficial effect of oAFMC in terms of osteogenic stimulation was less evident and ascribable to the slight increase in the thickness of the newly deposited bony tissue. However, while

after 90 days the scaffold was probably completely resorbed, thus stopping its osteoinductive role, by contrast, oAFMC persisted within the grafted sinuses. Several live oAFMC were, in fact, recorded within the implanted area 90 days after sinus lift, thus probably continuing to contribute to the process of host tissue remodeling. In addition, the presence of oAFMC modulated the inflammatory reaction induced by sinus lift procedures and by the insertion of scaffold within the maxillary cavity. This positive effect is in agreement with the peculiar biological properties showed by the different categories of placental-derived cells [24]. The placenta, thanks to its immunomodulatory activity and to low immunogenicity, forms a perfect interface between two immunologically distinct organisms, thus contributing to guarantee the maintenance of fetal–maternal tolerance during the pregnancy. These favorable immunological properties were conserved by all the categories of amniotic-derived cells, thus allowing two beneficial effects during their use in regenerative medicine. First of all, as indicated by an extensive literature [24], the low immunogenicity of amniotic-derived cells allowed their use into allo-xenogeneic settings into immunocompetent animals and without any immunosuppressive treatment [31]. In fact, the use of amniotic membrane as a therapeutic agent has been studied for decades in medicine for allogeneic treatment of skin wound, burn injuries, chronic leg ulcers, and for ocular surface reconstruction, thus extensively demonstrating its efficacy and safety [24]. More recently, the amnion has been investigated as a possible source of stem cells and the results of first clinical trials in human have proven that also the allogeneic transplantation of amniotic-derived cells in the absence of immunopressive treatment does not induce immunoreaction [55]. To reinforce these clinical evidences, various groups have experimented and demonstrated a prolonged survival of human amniotic membrane or amniotic-derived cells after xenogeneic transplantation into various immunocompetent animals and long-term engraftment after intravenous injection of heterogeneous human amniotic and chorionic cells into newborn swine or rats, with human microchimerism detected in several organs suggesting active migration and integration into specific organs and indicating active tolerance of the xenogeneic cells without any risk of teratoma [24]. Altogether, these evidences, combined with the *in vitro* studies providing the intimate mechanistic insight into the processes of tolerance vs. rejection of amniotic-derived cells [24], suggested this as ideal cell sources for the development of novel cell therapy procedures with reduced rates of rejection [24–31, 55]. This aspect is not surprising since the immunological phenotype of oAFMC is exactly similar to that described for human AFMC [31]. In particular, they displayed a weak expression of MHC I and the absence of MHC II antigens. The *in vitro* studies aimed to understand the mechanisms underlying the immunomodulatory effects observed after allo-xenogeneic transplantation of placenta-derived cells, showing that these cells actively

suppress T cell proliferation through the secretion of soluble immune-modulatory factors [56–58]. In addition, human AFMC are able to produce in vitro IL-6 and IL-8 [59, 60]. The presence of oAFMC with the engineered scaffold, in addition, modulated the major mechanism involved in the process of tissue healing. The presence of oAFMC, in fact, positively influenced the angiogenic response of the grafted district during the first interval of healing (45 days), thus driving the generation of a widespread blood vessel network and supporting a significantly higher PI. Then, both vascular remodeling and PI drastically dropped in the presence of cells becoming significantly lower than those recorded in sinus grafted with RegenOss® alone. This latter result may be indicative of a more rapid evolution in the process of tissue regeneration and representative of a major degree of maturation of sinus treated with oAFMC; however, this clearly demonstrated the persistence of the cell modulatory role for 90 days.

Conclusions

The results obtained in the present research, designed to follow a hierarchical approach where in vitro tests were combined with in vivo animal studies [56], clearly showed that a commercial MgHA/collagen-based scaffold (RegenOss®) used in preprosthetic reconstructive surgery improve its clinical therapeutic outcome in the presence of AFMC. For this reason, AFMC could be proposed as a valid alternative source of MSC suitable to potentiate the process of bone regeneration induced by the technique of sinus augmentation also demonstrated by radiographic and ultrasound examinations performed in the present study. In particular, AFMC may become an ideal cell candidate for tissue engineering strategies applied to maxilla facial surgery on the basis of their potential to reduce the bone integration period, support a robust mineralization for an extended period of time [6], and immunotolerate when allotransplanted into an immunocompetent patient [56–59].

Acknowledgments The authors gratefully acknowledge the help of Maura Turriani and Oriana Di Giacinto in providing precious technical support. This work was financed by Tercas Foundation, Teramo, Italy and supported by Fin-Ceramica Faenza S.p.A., Società della Tampieri Financial Group S.p.A, Faenza, Italy.

Conflict of interest None.

References

- Groeneveld EH, van den Bergh JP, Holzmann P, ten Bruggenkate CM, Tuinzing DB, Burger EH (1999) Mineralization processes in demineralized bone matrix grafts in human maxillary sinus floor elevations. *J Biomed Mater Res* 48:393–402
- Esposito M, Grusovin MG, Rees J, Karasoulos D, Felice P, Alissa R, Worthington HV, Coulthard P (2010) Interventions for replacing missing teeth: augmentation procedures of the maxillary sinus. *Cochrane Database Syst Rev* 17:CD008397.
- Aghaloo TL, Moy PK (2007) Which hard tissue augmentation techniques are the most successful in furnishing bony support for implant placement? *Int J Oral Maxillofac Implants* 22:49–70
- Browaeys H, Bouvry P, De Bruyn H (2007) A literature review on biomaterials in sinus augmentation procedures. *Clin Implant Dent Relat Res* 9:166–177
- Gutwald R, Haberstroh J, Kuschnierz J, Kister C, Lysek DA, Maglione M, Xavier SP, Oshima T, Schmelzeisen R, Sauerbier S (2010) Mesenchymal stem cells and inorganic bovine bone mineral in sinus augmentation: comparison with augmentation by autologous bone in adult sheep. *Br J Oral Maxillofac Surg* 48:285–290
- Pettinicchio M, Traini T, Murmura G, Caputi S, Degidi M, Mangano C, Piattelli A (2012) Histologic and histomorphometric results of three bone graft substitutes after sinus augmentation in humans. *Clin Oral Investig* 16:45–53
- Huang HL, Hsu JT, Chen MY, Liu C, Chang CH, Li YF, Chen KT (2012) Microcomputed tomography analysis of particular autogenous bone graft in sinus augmentation at 5 months: differences on bone mineral density and 3D trabecular structure. *Clin Oral Investig* 2012 Apr 25. [Epub ahead of print].
- Moore WR, Graves SE, Bain GI (2001) Synthetic bone graft substitutes. *ANZ J Surg* 71:354–361
- Nkenke E, Stelzle F (2009) Clinical outcomes of sinus floor augmentation for implant placement using autogenous bone or bone substitutes: a systematic review. *Clin Oral Implants Res* 20:124–33
- Vikram D, Nather A, Khalid KA (2005) Role of ceramics on bone graft substitutes. In: Nather A (ed) Bone grafts and bone substitutes: basic science and clinical applications. World Scientific, New Jersey, pp 445–458
- Abukawa H, Papadaki M, Abulikemu M, Leaf J, Vacanti JP, Kaban LB, Troulis MJ (2006) The engineering of craniofacial tissues in the laboratory: a review of biomaterials for scaffolds and implant coatings. *Dent Clin North Am* 50:205–216
- Palarie V, Bicer C, Lehmann KM, Zahalka M, Draenert FG, Kämmerer PW (2011) Early outcome of an implant system with a resorbable adhesive calcium-phosphate coating—a prospective clinical study in partially dentate patients. *Clin Oral Investig* 16:1039–1048
- Kühl S, Brochhausen C, Götz H, Filippi A, Payer M, d'Hoedt B, Kreisler M (2012) The influence of bone substitute materials on the bone volume after maxillary sinus augmentation: a microcomputerized tomography study. *Clin Oral Investig* Apr 27. [Epub ahead of print].
- Degidi M, Artese L, Rubini C, Perrotti V, Iezzi G, Piattelli A (2006) Microvessel density and vascular endothelial growth factor expression in sinus augmentation using Bio-Oss. *Oral Dis* 12:469–475
- Kasemo B (2002) Biological surface science. *Surf Sci* 500:656–677
- Deligianni DD, Katsala N, Ladas S, Sotiropoulou D, Amedee J, Missirlis YF (2001) Effect of surface roughness of the titanium alloy Ti-6Al-4V on human bone marrow cell response and on protein adsorption. *Biomaterials* 22:1241–1251
- Lamers E, Walboomers XF, Domanski M, te Riet J, van Delft FC, Luttge R, Winnubst LA, Gardeniers HJ, Jansen JA (2010) The influence of nanoscale grooved substrates on osteoblast behavior and extracellular matrix deposition. *Biomaterials* 31:3307–3316
- Mendonça G, Mendonça DB, Aragão FJ, Cooper LF (2010) The combination of micron and nanotopography by H(2)SO(4)/H(2)O (2) treatment and its effects on osteoblast-specific gene expression of hMSCs. *J Biomed Mater Res A* 94:169–179

19. Wahl DA, Czernuszka JT (2006) Collagen-hydroxyapatite composites for hard tissue repair. *Eur Cell Mater* 28:43–56
20. Tampieri A, Celotti G, Landi E, Sandri M, Roveri N, Falini G (2003) Biologically inspired synthesis of bone-like composite: self-assembled collagen fibers/hydroxyapatite nanocrystals. *J Biomed Mater Res A* 67:618–625
21. Kon E, Muttini A, Arcangeli E, Delcogliano M, Filardo G, Nicoli Aldini N, Pressato D, Quarto R, Zaffagnini S, Marcacci M (2010) Novel nanostructured scaffold for osteochondral regeneration: pilot study in horses. *J Tissue Eng Regen Med* 4:300–308
22. Tampieri A, Sprio S, Sandri M, Valentini F (2011) Mimicking natural bio-mineralization processes: a new tool for osteochondral scaffold development. *Trends Biotechnol* 29:526–535
23. Razzouk S, Schoor R (2011) Mesenchymal stem cells and their challenges for bone regeneration and osseointegration. *J Periodontol* 83:547–550
24. Parolini O, Soncini M, Evangelista M, Schmidt D (2009) Amniotic membrane and amniotic fluid derived cells; potential tools for regenerative medicine? *Reg Med* 4:275–291
25. Prusa AR, Hengstschlager M (2002) Amniotic fluid cells and human stem cell research: a new connection. *Med Sci Monit* 8: RA253–RA257
26. Prusa AR, Marton E, Rosner M, Bernaschek G, Hengstschlager M (2003) Oct-4-expressing cells in human amniotic fluid: a new source for stem cell research? *Hum Reprod* 18:1489–1493
27. In't Anker PS, Scherjon SA, Kleijburg-van der Keur C, Noort WA, Claas FH, Willemze R, Fibbe WE, Kanhai HH (2003) Amniotic fluid as a novel source of mesenchymal stem cells for therapeutic transplantation. *Blood* 102:1548–1549
28. Fauza D (2004) Amniotic fluid and placental stem cells. *Best Pract Res Clin Obstet Gynaecol* 18:877–891
29. Antonucci L, Stuppia L, Kaneko Y, Yu S, Tajiri N, Bae EC, Chheda SH, Weinbren NL, Borlongan CV (2011) Amniotic fluid as a rich source of mesenchymal stromal cells for transplantation therapy. *Cell Transplant* 20:789–795
30. Tsai MS, Lee JL, Chang YJ, Hwang SM (2004) Isolation of human multipotent mesenchymal stem cells from second-trimester amniotic fluid using a novel two-stage culture protocol. *Hum Reprod* 19:1450–1456
31. De Coppi P, Bartsch G Jr, Siddiqui MM, Xu T, Santos CC, Perin L, Mostoslavsky G, Serre AC, Snyder EY, Yoo JJ, Furth ME, Soker S, Atala A (2007) Isolation of amniotic stem cell lines with potential for therapy. *Nat Biotechnol* 25:100–106
32. McLaughlin D, Tsirimonaki E, Vallianatos G, Sakellaridis N, Chatzistamatiou T, Stavropoulos-Gioka C, Tsezou A, Messinis I, Mangoura D (2006) Stable expression of a neuronal dopaminergic progenitor phenotype in cell lines derived from human amniotic fluid cells. *J Neurosci Res* 83:1190–1200
33. Cipriani S, Bonini D, Marchina E, Balgkouranidou I, Caimi L, Grassi Zucconi G, Barlati S (2007) Mesenchymal cells from human amniotic fluid survive and migrate after transplantation into adult rat brain. *Cell Biol Int* 31:845–850
34. Peister A, Woodruff MA, Prince JJ, Gray DP, Huttmacher DW, Guldberg RE (2011) Cell sourcing for bone tissue engineering: amniotic fluid stem cells have a delayed, robust differentiation compared to mesenchymal stem cells. *Stem Cell Res* 7:17–27
35. Antonucci I, Iezzi I, Morizio E, Mastrangelo F, Pantalone A, Mattioli-Belmonte M, Gigante A, Salini V, Calabrese G, Tetè S, Palka G, Stuppia L (2009) Isolation of osteogenic progenitors from human amniotic fluid using a single step culture protocol. *BMC Biotechnol* 9:9. doi:10.1186/1472-6750-9-9
36. Chen Q, Xiao P, Chen JN, Cai JY, Cai XF, Ding H, Pan YL (2010) AFM studies of cellular mechanics during osteogenic differentiation of human amniotic fluid-derived stem cells. *Anal Sci* 26:1033–1037
37. De Rosa A, Tirino V, Paino F, Tartaglione A, Mitsiadis T, Feki A, d'Aquino R, Laino L, Colacurci N, Papaccio G (2011) Amniotic fluid-derived mesenchymal stem cells lead to bone differentiation when cocultured with dental pulp stem cells. *Tissue Eng Part A* 17:645–653
38. Sun H, Feng K, Hu J, Soker S, Atala A, Ma PX (2010) Osteogenic differentiation of human amniotic fluid-derived stem cells induced by bone morphogenetic protein-7 and enhanced by nanofibrous scaffolds. *Biomaterials* 31:1133–1139
39. Peister A, Porter BD, Kolambkar YM, Huttmacher DW, Guldberg RE (2008) Osteogenic differentiation of amniotic fluid stem cells. *Biomed Mater Eng* 18:241–246
40. Bossolasco P, Montemurro T, Cova L, Zangrossi S, Calzarossa C, Buiatitios S, Soligo D, Bosari S, Silani V, Deliliers GL, Rebulla P, Lazzari L (2006) Molecular and phenotypic characterization of human amniotic fluid cells and their differentiation potential. *Cell Res* 16:329–336
41. Antonucci I, Pantalone A, De Amicis D, D'Onofrio S, Stuppia L, Palka G, Salini V (2009) Human amniotic fluid stem cells culture onto titanium screws: a new perspective for bone engineering. *J Biol Regul Homeost Agents* 23:277–279
42. Estaca E, Cabezas J, Usón J, Sánchez-Margallo F, Morell E, Latorre R (2008) Maxillary sinus-floor elevation: an animal model. *Clin Oral Implants Res* 19:1044–1048
43. Colosimo A, Curini V, Russo V, Mauro A, Bernabò N, Marchisio M, Alfonsi M, Muttini A, Mattioli M, Barboni B (2012) Characterization, GFP gene nucleofection and allotransplantation in injured tendons of ovine amniotic fluid-derived stem cells. *Cell Transplantation* Apr 10. [Epub ahead of print].
44. Mattioli M, Gloria A, Turriani M, Mauro A, Curini V, Russo V, Tetè S, Marchisio M, Pierdomenico L, Berardinelli P, Colosimo A, Muttini A, Valbonetti L, Barboni B (2011) Stemness characteristics and osteogenic potential of sheep amniotic epithelial cells. *Cell Biol Int* 36:7–19
45. Muttini A, Mattioli M, Petrizzi L, Varasano V, Sciarrini C, Russo V, Mauro A, Coccione D, Turriani M, Barboni B (2010) Experimental study on allografts of amniotic epithelial cells in calcaneal tendon lesions of sheep. *Vet Res Commun* 34:S117–S120
46. Barboni B, Russo V, Curini V, Mauro A, Martelli A, Muttini A, Bernabò N, Valbonetti L, Marchisio M, Di Giacinto O, Berardinelli P, Mattioli M (2012) Achilles tendon regeneration can be improved by amniotic epithelial cells allotransplantation. *Cell Transplant*. doi:10.3727/096368912X638892
47. Martelli A, Palmerini MG, Russo V, Rinaldi C, Bernabò N, Di Giacinto O, Berardinelli P, Nottola SA, Macchiarelli G, Barboni B (2009) Blood vessel remodeling in pig ovarian follicles during the periovulatory period: an immunohistochemistry and SEM-corrosion casting study. *Reprod Biol Endocrinol* (7):72
48. Martelli A, Bernabò N, Berardinelli P, Russo V, Rinaldi C, Di Giacinto O, Mauro A, Barboni B (2009) Vascular supply as a discriminating factor for pig preantral follicle selection. *Reproduction* 137:45–58
49. Barboni B, Martelli A, Berardinelli P, Russo V, Turriani M, Bernabò N, Lucidi P, Mattioli M (2004) Ovarian follicle vascularization in fasted pig. *Theriogenology* 62:943–957
50. d'Aquino R, Graziano A, Sampaolesi M, Laino G, Pirozzi G, De Rosa A, Papaccio G (2007) Human postnatal dental pulp cells co-differentiate into osteoblasts and endotheliocytes: a pivotal synergy leading to adult bone tissue formation. *Cell Death Differ* 14:1162–1171
51. Laino G, d'Aquino R, Graziano A, Lanza V, Carinci F, Naro F, Pirozzi G, Papaccio G (2005) A new population of human adult dental pulp stem cells: a useful source of living autologous fibrous bone tissue (LAB). *J Bone Miner Res* 20:1394–1402
52. d'Aquino R, De Rosa A, Lanza V, Tirino V, Laino L, Graziano A, Desiderio V, Laino G, Papaccio G (2009) Human mandible bone

- defect repair by the grafting of dental pulp stem/progenitor cells and collagen sponge biocomplexes. *Eur Cell Mater* 18:75–83
53. Spath L, Rotilio V, Alessandrini M, Gambarà G, De Angelis L, Mancini M, Mitsiadis TA, Vivarelli E, Naro F, Filippini A, Papaccio G (2010) Explant-derived human dental pulp stem cells enhance differentiation and proliferation potentials. *J Cell Mol Med* 14:1635–1644
54. Mangano C, Paino F, d'Aquino R, De Rosa A, Iezzi G, Piattelli A, Laino L, Mitsiadis T, Desiderio V, Mangano F, Papaccio G, Tirino V (2011) Human dental pulp stem cells hook into biocoral scaffold forming an engineered biocomplex. *PLoS One* 6:e18721
55. Evangelista M, Soncini M, Parolini O (2008) Placenta-derived stem cells: new hope for cell therapy? *Cytotechnology* 58:33–42
56. Wolbank S, Peterbauer A, Fahrner M, Hennerbichler S, van Griensven M, Stadler G, Redl H, Gabriel C (2007) Dose dependent immunomodulatory effect of human stem cells from amniotic membranes: a comparison with human mesenchymal stem cells from adipose tissue. *Tissue Eng* 13:1173–1183
57. Magatti M, De Munari S, Vertua E, Gibelli L, Wengler GS, Parolini O (2008) Human amnion mesenchyme harbors cell with allogeneic T cell suppression stimulation capacity. *Stem cell* 26:182–192
58. Banas RA, Trumpower C, Bentlejewski C, Marshall V, Sing G, Zeevi A (2008) Immunogenicity and immunomodulatory effects of amnion derived multipotent progenitor cells. *Human Immunol* 69:321–328
59. Mazzucchelli I, Avanzini MA, Ciardelli L, Pagani S, Greco R, Belloni C, Castellazzi A, Marconi M, Rondini G, Polatti F (2004) Human amniotic fluid cells are able to produce IL-6 and IL-8. *Am J Reprod Immunol* 51:198–203
60. Yan WH, Lin A, Chen XJ, Dai MZ, Xu HH, Chen BG, Gan LH, Shi WW (2008) Immunological aspect of human amniotic fluid cells: implication for normal pregnancy. *Cell Biol Intern* 32:93–99

Copyright of Clinical Oral Investigations is the property of Springer Science & Business Media B.V. and its content may not be copied or emailed to multiple sites or posted to a listserv without the copyright holder's express written permission. However, users may print, download, or email articles for individual use.